Angular Power Distribution Measurements and Modelling of Outdoor Urban Environment Using Ray-tracing At 2 and 18 GH

Hejselbæk, Johannes; Karstensen, Anders; Pedersen, Gert F.

Published in:
2016 10th European Conference on Antennas and Propagation (EuCAP)

DOI (link to publication from Publisher):
10.1109/EuCAP.2016.7481354

Publication date:
2016

Document Version
Accepted author manuscript, peer reviewed version

Angular Power Distribution Measurements and Modeling of Outdoor Urban Environment using Ray-tracing at 2 and 18 GHz

Johannes Hejselbæk, Anders Karstensen, Gert Frølund Pedersen
Department of Electronic Systems, Faculty of Engineering and Science, Aalborg University, Denmark
Email: {joh, andka, gfp}@es.aau.dk

***Abstract*—In order to enable the fifth generation of mobile communication (5G), understanding of the expected radio channel is needed. This is to enable modeling of the radio environment to use in network planning and development. Due to this, channel measurements were conducted at 18 GHz and 2 GHz for comparison of angular power distribution. The chosen environment for the measurement is an outdoor urban scenario with a transmitting base-station at rooftop level and a receiver at ground level. The measurements show that the propagation environment becomes more directive at 18 GHz compared to 2 GHz. Simulations using a commercial ray-tracing tool highlight areas of further development of ray-tracing tools to ensure agreement between simulations and measurements.**

***Index Terms*—centimeter-wave, channel modeling, channel measurement, 5G, angular power distrubution, ray-tracing.**

I. INTRODUCTION

The mobile industry is moving towards a fifth generation mobile network (5G) [1]. Cisco predicts that the global mobile data traffic will increase nearly tenfold between 2014 and 2019 [2]. This increase in volume comes together with a demand for higher data rates at the end user. To facilitate this there is a need for more bandwidth [3]. The availability of unused bandwidth is limited at the current frequency range, which is why there is great interest in exploiting the centimeter and millimeter wave bands (10-90GHz) [4].

One of the challenges in the development of 5G systems is the lack of channel models developed for some of these higher frequencies. For the unlicensed frequency band at 60 GHz, used for IEEE 802.11ad, there are significant available studies [5]. The IEEE 802.11ad standard is for short range indoor to indoor communication. For the outdoor to outdoor and outdoor to indoor long-range communication, there are fewer available models. The available models relate to point to point systems (Microwave Links), which today is mostly used for line-of-sight communication as described in ITU-R P530-16. However if these frequencies are to be used for 5G and thereby also in a non-line of sight (NLOS) scenario, the propagation paths experienced in a mobile channel have to be described. Path losses (including free space losses, atmospheric absorption, penetration losses, etc.) are, to some extent, described by ITU P1410-5 and ITU-R P676-10 more in direct relation to 5G also in [6]. The transmission loss becomes significant at these high frequencies (20-40dB) which is why outdoor to indoor systems is not expected for a 5G system [7]. Focus for this work has been on outdoor to outdoor propagation in a NLOS scenario.

The mechanisms behind the electromagnetic wave interactions are diverse, but can generally be divided to reflection, diffraction, and scattering. In ITU P1410-5 recommendations are presented for modeling of these for frequencies between 3 and 60 GHz. Also specific 5G channel models have been presented as in [8]. These models are the basis for simulation tools like ray-tracing. Measurements have been conducted to validate some of the models for some frequencies. As mentioned 60 GHz have been studied and more relevant for 5G also 28 and 38 GHz as presented in [9, 10, 11]. However, there is still a need for further studies in order to capture and describe some of the electromagnetic mechanisms.

The interest in modeling all the mechanisms correctly is based on the impact it has on the angle of arrival (AoA) of the signal at the receiver. This is important as the proposed frequencies for 5G are in the higher centimeter and the millimeter wave bands. This limits the range of conventional sectorial mobile systems and therefore beam steering is suggested as an enabling technology [12]. The use of the beam steering is possible both at the base-station and mobile terminal as the short wavelengths makes it possible to fit directive antenna arrays using a small form factor. The use of adaptive beam-steering starts posing a new dimension for the planning of conventional sectorial mobile systems. This is why the AoA at the mobile terminal is now an important factor. Network planners often turns to map-based ray-tracing and therefor these tools have to be able to model the AoA which can pose a challenge to their capability [13].

The aim of this paper is to describe one method for recording the angular power distribution using directive antennas. The recorded angular power distributions at 2 and 18 GHz are then compared. Following this, the scenario is modeled in the ray-tracing tool Wireless InSite from REMCOM. Results from running simulations in the tool using different parameters is then compared to the recorded angular power distribution.

This paper is organized as follows. Section II describes the measurement setup and presents the recorded angular power distribution. Section III describes the modeling using the ray-tracing tool and compares the simulations to the recorded angular power distributions. Section IV summarizes this work.

II. Angular Power Distribution measurements

The purpose of this measurement campaign is to investigate the difference in angular power distribution at 2 and 18GHz. Due to limitations in the available equipment there was an upper frequency limit of 18 GHz. The intentions is to visualize the difference in AoA of power at the two frequencies.

A. Measurements Setup

The measurements was conducted using a transmitting 'base station' (TX) located at the roof of a building as shown in Fig. 1. The receiver (RX) was mounted on an automated rotation rig located at ground level. The height difference between TX and RX was 11.5 m. The placement and height of TX and RX site were chosen to force NLOS. This was chosen as the interactions between TX and RX was the subject of interest. The distance between the two sites was 42 m. A 360-degree panoramic picture of the surroundings is shown in Fig. 3.

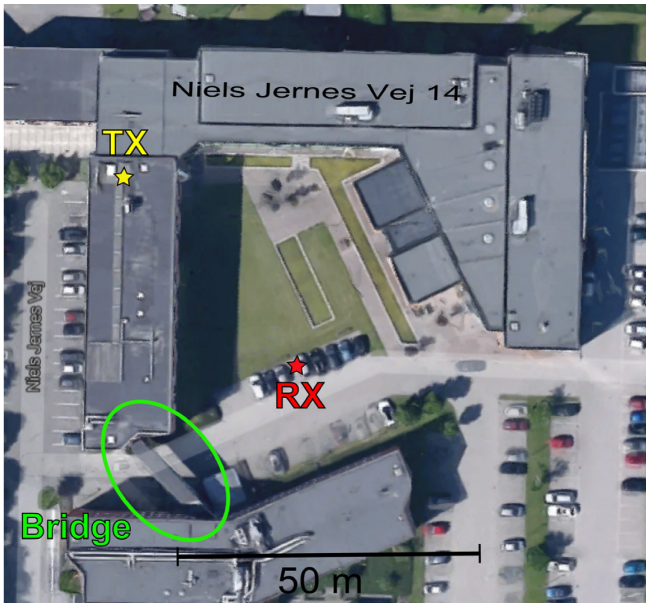

Fig. 1. Top view map of the location of the measurement. [Google Map]

The measurement system was composed of two parallel systems, one for 2 GHz and another for 18 GHz. At the TX site two EMCO 31115 horn antennas where used. These were in azimuth oriented towards the RX site. In elevation, they were tilted slightly towards the edge of the building between TX and RX site. The half power beam width (HPBW) of the EMCO horn in the azimuth plane (ϕ) is for 2 GHz 55^o and for 18 GHz 10^o. Two signal generators with additional amplification was used for the two RF chains. These were transmitting a continuous wave (CW) with bandwidth 10MHz and 100MHz for respectively 2 and 18 GHz. The maximum effective radiated power (ERP) for 2 GHz was 48 dBm, and for 18 Ghz the maximum ERP was 42 dBm.

At the RX site, a COMSAT PCND085 antenna was used for the 2 GHz signal which have a ϕ HPBW of 5^o. For the 18 GHz signal, a BBHA 9120D horn antenna with ϕ HPBW of 10^o was used. The RX antennas was in elevation oriented leveled, with the ground as reference. In azimuth they were rotated a full 360^o in steps of 2.5^o using a fully automated turntable rig, as seen in Fig. 2. The power spectrum was recorded using two spectrum analyzers, one for each frequency. For 2 GHz a R&S FSL6 was used and for 18 GHz a R&S FSEM 30.

Fig. 2 Rotation rig with receiver antennas and spectrum analyzers

The measurement was conducted during the night were it was possible to close of the entire courtyard seen in Fig. 1. This was done in order to ensure a static environment. A full rotation was divided in to 144 measurements, which in total took approximately one hour.

B. Measurements result

The measured angular power distribution for both 2 and 18 GHz is plotted in Fig. 3. The two traces from are compared to the surroundings by using a 360° panorama picture taken from the position of the receiver. It should be noted that in order to make the orientation of the picture fit with the plot, the x-axis of the plot is flipped in order to follow the direction of the rotation in the measurements.

Fig. 3 shown that the power for the 2 GHz trace is distributed over the entire angular spectrum. The 18 GHz trace shows that the power is concentrated around one main direction. From this it can be concluded that the propagation environment for the 2 GHz is not directive and that the 18 GHz is behaving directive. The introduction of defectiveness at 18 GHz is mainly due to the higher free-space losses between antennas and a narrower pattern at the transmitter. This higher loss results in the rays attenuating faster, giving that only a low number of ray interactions can occur before the power is below the receiver sensitivity.

When Fig. 3 is investigated further and the plot is compared to the map, it is possible to find power peaks that correspond well with the geometry of the scenario. For the 2GHz curve close to 90° (1) the maximum peek is found. This could correspond to a single reflection from the glass wall. Close to this at 60° (2) a strong peak is seen which correspond to a single reflection from the brick wall. At 295° (3) the reflection from the wall behind the receiver, relative to the transmitter, is found. For the 18 GHz trace some of the same

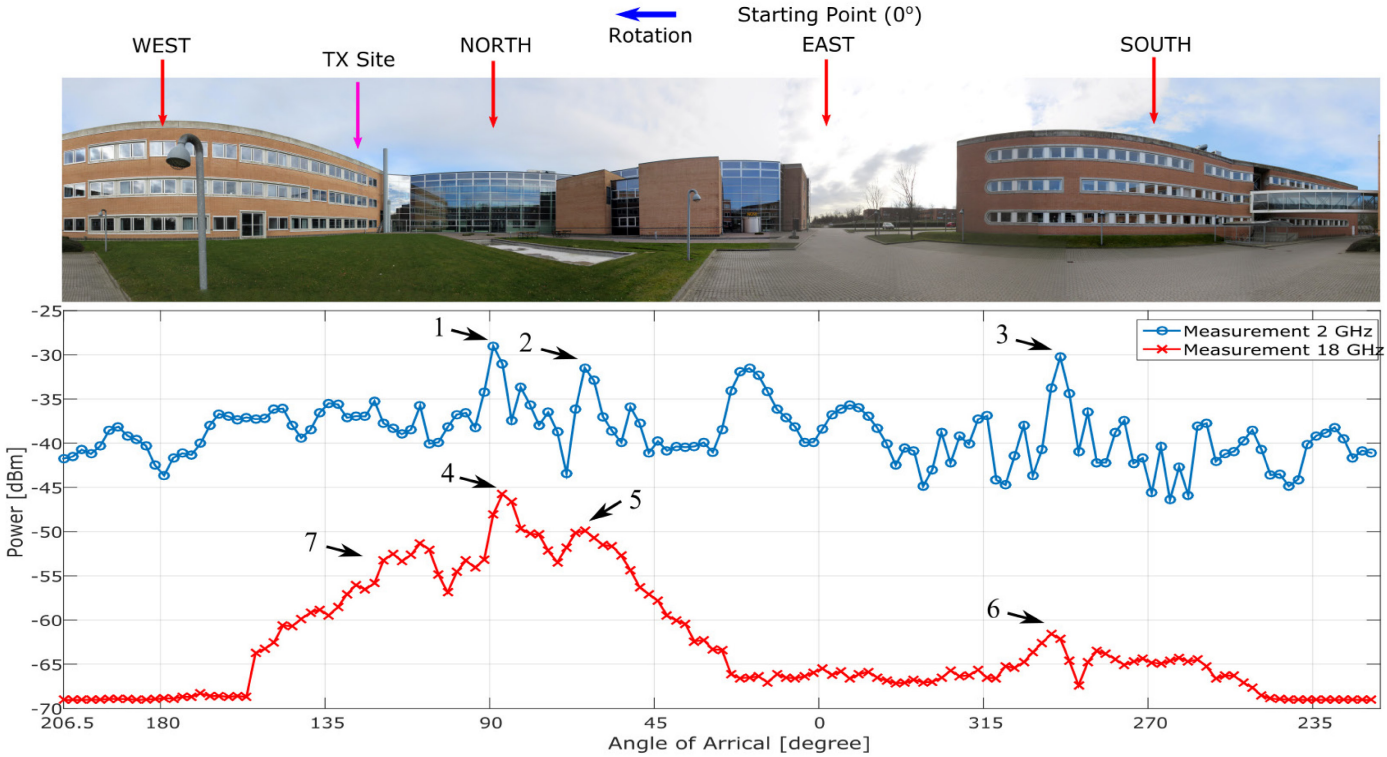

Fig. 1 Measured angular power distribution plotted with 360-degree panoramic picture of the surroundings.

component as for the 2 GHz trace can be found. The maximum peak also located close to 90° (4) is presumed to be a reflection from the glass wall north of the receiver and then to the receiver. The lope from 20° to 60° (4) could correspond to reflections from the brick/glass wall. The peak at 295° (6) is the reflection from the wall behind the receiver. The lobe from 110° to 150° (7) could be diffraction from the edge of the roof between TX and RX site.

From the found relations between measurements and the surroundings is it found that some of these can be used at reference points for the following modeling using ray-tracing.

III. MODELING USING RAY-TRACING

The modeling in the used ray-tracing tool is map based. The used map is extracted from information from the Danish Geodata Agency and aerial photos. The resulting map shown in Fig. 4.

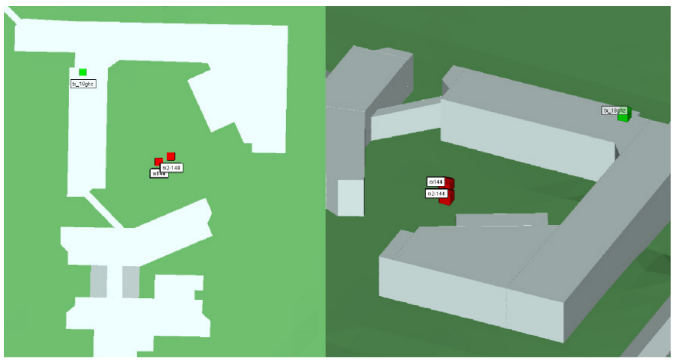

Fig. 4 Wireless InSide map and perspective view

In the map, shown left in Fig. 4, the TX and RX site is placed shown by the red and green dots. The green dot is the TX site and the red the RX site. Note that there here is shown two red RX positions. This is due to an alternative position, which also was measured and simulated. The difference between the results from the alternative position and the ones presented where however not significant and therefore not presented here. In order to provide the best possible data for the position and elevation of the measurement points a surveyor grade GPS system was used. In specific a Leica GPS1200 which uses RTK corrections in order to achieve an accuracy of centimeters.

When using map base models of the surroundings simplifications are made to the structures. The can be seen in Fig. 4, especially the perspective view to the right. Here it is clear how the buildings are simplified to smooth surfaces. The chosen simplifications follows the approach used for large scale network planning. Due to this, it is also chosen to model all the surfaces using the same material. This as a total database describing all buildings not can be expected. This method where a 2D map is transformed to a 3D map is not able to catch 'floating' structures as the bridge marked in Fig. 1 and seen in the top right corner of Fig. 3. The impact of this is to be investigated.

For the simulation the antenna patterns are included for each individual antenna. The antenna patterns are an important factor in order to be able to compare the simulations with the measurements. Due to this a study and measurement campaign of the radiation patterns for all the used antennas have been conducted. This is however not covered by this paper. The used ray-tracing tool enables the patterns to be

imported and the resulting received power at the measurement points is therefore comparable to the one of the horn antennas, used for the measurement.

The resulting angular power distributions from the simulation tool are presented in Fig. 5 and Fig. 6 for 2 and 18 GHz respectively.

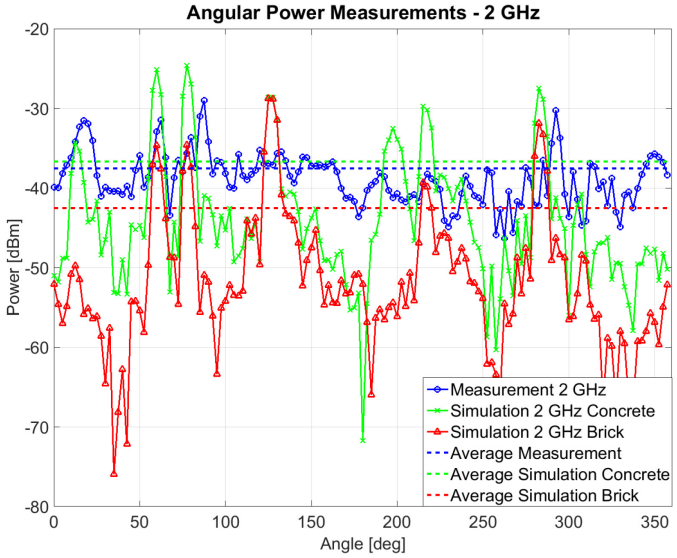

Fig. 5 Angular power distribution for 2 GHz

In Fig. 5 the measurements are plotted together with the simulated angular power distribution for both *concrete* and *brick*. These two refer to the chosen material for the buildings which is based on standard material (*concrete*) from the ray-tracing tool and a tuned material (*brick*) based on [15]. The parameters for the two are shown in TABLE II.

TABLE I. MATERIAL CONSTANTS

Material	***f*** [GHz]	**σ** [S/m]	**ε_r** [F/m]	Thickness [m]
Concrete	2 and 18	0.015	15	0.3
Brick	2	0.0173	4.50	0.3
Brick	18	0.0364	4.11	0.3

As seen in Fig. 5 the tuned *brick* materials average power is closer to the average received power of the measurement. This indicate that the tuned material performs better in the simulation. It can also be seen that there is a discrepancy between the measured strongest DOA and the simulated. The simulation predicts the strongest DOA to be from the diffracted path over the edge of the building between TX and RX and the reflection back from behind the RX site seen from the TX site. The brick and concrete correlations to the measurement are respectively 0.20 and 0.25. These are both very low correlations and confirms that it is difficult to relate the peaks and curves of the plot.

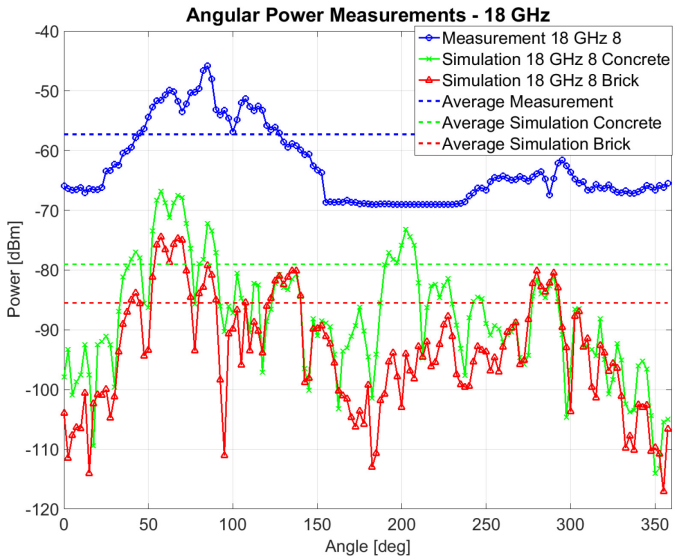

Fig. 6 Angular power distribution for 18 GHz

For the 18 GHz simulation shown in Fig. 6 it can be seen that there is a large difference between the average measured power and the simulated. However, it seems that the angular power distribution is following same trends. For 18 GHz, the brick and concrete correlations are respectively 0.56 and 0.44. These are higher values than for 2 GHz, but it is not considered a high level of correlation. An interesting finding from Fig. 6 is the peak for the concrete simulation shown at 200° which correspond to the end of the wall west of the receiver. This gives a strong reflection when the concrete material is used. Also next to this at approximately 215° is a strong peak which correspond to the bridge between the two buildings. These is not seen in the measurements, as there is a mismatch between the physical placement of bridge and the map model. The lower peaks in the simulation using brick as material can be caused by the difference in Brewster angle the material constants causes.

The offset in average power for 18 GHz is studied further by changing material constants to look for a better fit. Both the relative permittivity (ε_r) and conductivity is (σ) simulated using changing values. Changing ε_r from 4.11 to 12.5 and keeping σ = 0.01 did not give any significant change in the average power. Changing σ from 0.01 to ∞ (PEC) and keeping ε_r = 4.11, however did show a large difference. This is shown in Fig. 7. Here it is seen that modeling the surroundings using PEC gives a average power much closer to the measured. This could indicate that there is a need of looking further in to the way the materials are modeled in the simulation tool. Obviously, there is a need to investigate the different models behind the mechanism involved in the propagation from TX to RX in order to fully understand the resulting simulations.

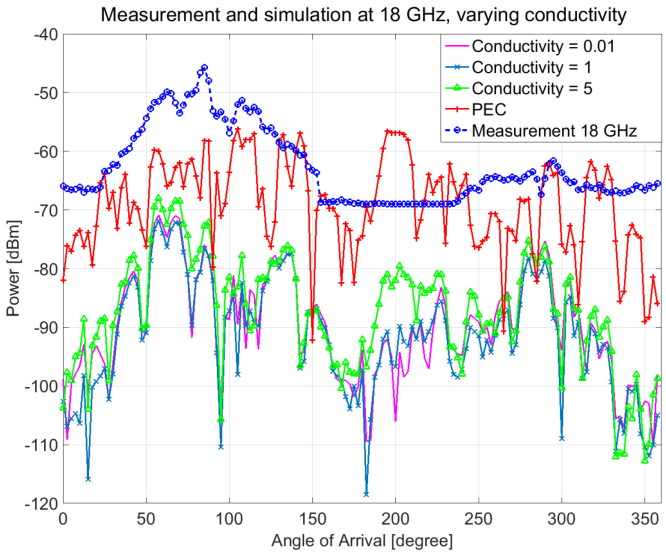

Fig. 7 Varying conductivity for simulation at 18 GHz

IV. CONCLUSION

This paper presents measurements for the angular power spectrum at 2 and 18 GHz for an outdoor urban scenario. The resulting angular power distribution shows, as expected, that the propagation environment becomes more directive at the higher frequency. The measured scenario is modeled using a commercial ray-tracing tool. The simulations shows that prediction of the angular power distribution is difficult at 2 GHz but seems to be possible at 18 GHz. The simulations also showed that the computed average received power is far of the measured at 18 GHz. This is expected to be caused by the internal used models in the simulation tool. A further study of this is planned for the future.

V. ACKOWLEDGMENT

The work have been conducted under the framework of the VIRTUOSO project. The Danish National Advanced Technology Foundation supports this project.

VI. REFERENCES

[1] P. Demestichas, A. Georgakopoulos, D. Karvounas, K. Tsagkaris, V. Stavroulaki, J. Lu, C. Xiong and J. Yao, "5G on the Horizon," *IEEE vehicular technology magazine,* Vols. 1556-6072, pp. 47-53, 2013.

[2] CISCO, "Global mobile data traffic will increase nearly tenfold between 2014 and 2019.," CISCO Whitepaper, 2015.

[3] L. Qian, N. Huaning, P. Apostolos and G. Wu, "5G Network Capacity - Key Elements and Technologies," *IEEE vehicular technology magazine,* vol. 14, pp. 1556-6072, 2014.

[4] The METIS Project, "Mobile and wireless communications Enablers for the Twenty-twenty Information Society," 2015.

[5] A. Maltsev, R. Maslennikov, A. Sevastyanov, A. Khoryaev and A. Lomayev, "Experimental Investigations of 60 GHz WLAN Systems in Office Environment," *IEEE Journal on Selected Areas in Communications,* vol. 27, no. 8, pp. 1488-1499, 2009.

[6] A. Sulyman, A. Nassar, M. Samimi, G. MacCartney, T. Rappaport and A. Alsanie, "Radio Propagation Path Loss Models for 5G Cellular Networks in the 28 GHz and 38 GHz Millimeter-Wave Bands," *IEEE Communications Magazine ,* vol. 52, no. 8, pp. 78-86, Sep. 2014.

[7] C.-X. Wang, F. Haider, X. Gao, X.-H. You, Y. Yang, D. Yuan, H. M. Aggoune, H. Haas, S. Fletcher and E. Hepsaydir, "Cellular Architecture and Key Technologies for 5G Wireless Communication Networks," *IEEE Communications Magazine,* vol. 52, no. 2, pp. 122-130, 2014.

[8] P. Kyösti and J. Medbo, "A channel model for 5G evaluations," in *COST-IC1004*, Dublin, Ireland, 2015.

[9] T. s. Rappaport, S. Sun, R. Mayzus, H. Zhao, Y. Azar, K. Wang, G. N. Wong, J. K. Schulz, M. Samimi and a. F. Gutierrez, "Millimeter Wave Mobile Communications for 5G Cellular: It Will Work!," *IEEE Access,* vol. 1, no. 2169-3536, pp. 335-349, 2013.

[10] T. S. Rappaport, J. Felix Gutierrez, E. Ben-Dor, J. N. Murdock, Y. Qiao and J. I. Tamir, "Broadband Millimeter-Wave Propagation Measurements and Models Using Adaptive-Beam Antennas for Outdoor Urban Cellular Communications," *IEEE Transactions On Antennas And Propagation,* vol. 61, no. 4, pp. 1850-1859, 2013.

[11] S. Rangan, T. S. Rappaport and E. Erkip, "Millimeter-Wave Cellular Wireless Networks: Potentials and Challenges," *Proceedings of the IEEE,* vol. 102, no. 3, pp. 366-385, 2014.

[12] W. Roh, J.-Y. Seol, J. Park, B. Lee, J. Lee, Y. Kim, J. Cho, K. Cheun and F. Aryanfar, "Millimeter-Wave Beamforming as an Enabling Technology for 5G Cellular Communications: Theoretical Feasibility and Prototype Results," *IEEE Communications Magazine,* vol. 52, no. 2, pp. 106-113, Feb. 2014.

[13] T. Fügen, J. Maurer, T. Kayser and W. Wiesbeck, "Capability of 3-D Ray Tracing for Defining Parameter Sets for the Specification of Future Mobile Communications Systems," *IEEE Transactions on Antennas and Propagation,* vol. 54, no. 11, pp. 3125-3136, 2006.

[14] Z. Zhang, Z. Yun and M. Iskander, "New computationally efficient 2.5D and 3D Ray Tracing Algorithms for modeling propagation environments," in *Antennas and Propagation Society International Symposium, 2001. IEEE* , Boston, USA, IEEE.

[15] C. D. Taylor, S. J. Gutierrez, S. L. Langdon, K. L. Murphy and W. A. Walton, "Measurement of RF Propagation into Concrete Structures over the Frequency Range 100 MHz ro 3 GHz," Phillips Laboratory - Documentation of Measurement Campaign, 1997.